Towards a strengthening of the coupling of numerical weather prediction and chemistry models to improve the retrieval of thermodynamic fields from infra-red passive sounders: the ozone case

Olivier COOPMANN*[1], Vincent GUIDARD†[1], et Nadia FOURRIÉ ‡[1]

[1]CNRM - Météo-France & CNRS, GMAP/OBS, Toulouse, France

February 26, 2018

Abstract

Hyper-spectral infra-red sensors on board polar-orbiting satellites provide 70 % (IASI-A and IASI-B alone account for 46 %) of the measurements used in the operational Numerical Weather Prediction (NWP) global model ARPEGE (Action de Recherche Petite Échelle Grande Échelle) of Météo-France. The infra-red passive sounding is sensitive to surface parameters and to many atmospheric constituents. The atmospheric temperature information is retrieved from those channels which are sensitive to gases and for which a prior knowledge of the vertical distribution is known. Most algorithms for infrared satellites measurements use carbon-dioxyde (CO_2) sensitive channels to retrieve temperature information. Parts of the infrared spectrum are also sensitive to ozone (O_3) but are not currently used in the NWP models of Météo-France. In the current version of the assimilation in the ARPEGE model, the gas concentrations used for the radiance simulations are considered constant in space and in time. However, a previous study showed that using realistic ozone information from the Chemistry Transport Model (CTM) MOCAGE (Modèle de Chimie Atmosphérique À Grande Échelle) of Météo-France as input of the Radiative Transfer Model improved temperature retrievals from infra-red satellites. The current study describes how the addition of IASI ozone-sensitive channels improves thermodynamic retrievals. An One Dimensional Variational data assimilation (1D-Var) framework allows to take into account error correlations between temperature, humidity and ozone from observation and background by means of the Desroziers method and to retrieve simultaneously thermodynamic variables and ozone by adding ozone in control vector.

Key-words: PNT, CTM, Ozone, Radiative Transfer Model, Data Assimilation, IASI.

*olivier.coopmann@umr-cnrm.fr
†vincent.guidard@meteo.fr
‡nadia.fourrie@meteo.fr

1 Introduction

Since the launch in 1960 of the first weather satellite, techniques have significantly evolved with ever more sophisticated instruments. Data from space borne intruments which are assimilated in NWP systems have a positive impact on forecasts [Hilton et al., 2012], [Lorenc and Marriott, 2014]. Hyper-spectral infra-red sounding instruments, such as the Atmospheric Infrared Sounder (AIRS), the Infra-red Atmospheric Sounding Interferometer (IASI) and the Cross-Track Infrared Sounder (CrIS), provide 70 % of the data used in the NWP global model ARPEGE (Action de Recherche Petite Échelle Grande Échelle) of Météo-France [Courtier et al., 1994]. IASI was jointly developed by CNES (Centre National d'Études Spatiales) and EUMETSAT (European Organisation for the Exploitation of Meteorological Satellites) [Cayla, 2001]. It was first launched in 2006 onboard the Metop-A satellite, the second instrument was launched on board Metop-B in 2012. Its spectrum ranges from 645 to 2760 cm^{-1} with a spectral sampling of 0.25 cm^{-1} and a spectral resolution of 0.5 cm^{-1} leading to a set of 8461 radiances at the top of the atmosphere. This sounder allows to obtain indirect information on temperature and humidity profiles and also on cloud cover, aerosols, atmospheric chemistry compounds such as O_3, CO_2, CO, CH_4, HNO_3 and N_2O [Clerbaux et al., 2009] and surface properties. The retrieval precision aimed at is 1 K/1 km for temperature and 10 %/1 km for humidity. This accuracy for temperature is achieved over oceans but there is room for improvement over continental surfaces and for humidity in the lower atmosphere that could come from better cloud detection techniques. The IASI instrument is fitted with an infra-red imaging radiometer which allows to coregister interferometric measurements with AVHRR (Advanced Very High Resolution Radiometer, present on the same platform) also providing cloud information [Saunders and Kriebel, 1988]. In this work, we first consider a channel selection that was performed

by [Collard, 2007], for NWP purposes. Channels were mainly chosen in the CO_2 long wave (LW) band (for temperature retrievals), in the atmospheric window region and in the water vapour (WV) band. This selection of 314 channels also included 15 ozone-sensitive channels. CNES added 14 other channels for monitoring purposes. This subset of 314 channels is routinely monitored at Météo-France and up to 123 channels are assimilated in operations (99 temperature channels in the LW CO_2 band, 4 window channels and 20 WV channels). The Global Telecommunication System (GTS) also distributes a set of 500 channels [Martinet et al., 2014] which includes the 314-channels subset. The objective of the present study is to improve thermodynamic retrievals from IASI data using realistic ozone information and the 15 ozone-sensitive channels available at Météo-France. In Section 2, the realism of two different ozone information is assessed, viz a climatology from RTTOV model (Radiative Transfer for TOVS)(TOVS: TIROS Operational Vertical Sounder and TIROS: Television Infra-Red Observation Satellite) hereafter referenced as RCLIM and an ozone field, provided by the French Chemistry Transport Model (CTM) [Sic et al., 2015] MOCAGE (MOdèle de Chimie Atmosphérique à Grande Échelle) here after referenced as MOC60L. This Section describes sensitivity of brightness temperature simulations to ozone information in a one dimensional framework using the variational formalism of data assimilation. In this section, the collocation and filtering techniques between radiosondes and IASI pixels are also explained. Both sources of information for ozone (RCLIM and MOC60L) are used as input of the Radiative Transfer Model (RTM) RTTOV and simulations are compared to real IASI observations. In section 3, the methodology, data which were used in the 1D-Var assimilation experiments using both sources of information for ozone and results with the 123 operational channels, with the addition of 15 ozone sensitive channels and with ozone in the control variable are developed further. Finally, conclusions and discussion are presented.

2 Sensitivity of simulations to ozone informations

Operationally at Météo-France, the IASI ozone-sensitive channels that are monitored range from 1014.5 to 1062.5 cm^{-1} (Table 1). The first source of information for ozone emanates from a climatological profile (RCLIM), which is constant in time and space with 101 levels up to 0.005 hPa and used operationally at Météo-France. This profile results from averaging a set of 83 diverse profiles from ECMWF (European Centre for Medium-Range Weather Forecast) analyses on 91 levels, interpolated to 101 levels [Chevallier et al., 2006]. The second source of ozone information available at Météo-France is a realistic field from the model MOCAGE (MOC60L) having 60 vertical hybrid sigma-pressure levels from the surface up to about 0.01 hPa and which takes into account the atmospheric chemical reactions describing the sources and sinks in time and space on a 2 ° global grid. The dynamics within the CTM are forced by ARPEGE meteorological analysis fields (pressure, winds, temperature, specific humidity) [Sic et al., 2015]. Figure 1.a shows an example of the ozone value for RCLIM at around 20 hPa level, and figure 1.b the field from MOCAGE at around the same pressure level. A constant ozone concentration of around 6 $ppmv$ is observed all over the globe with RCLIM while values of ozone concentration from MOC60L vary in space between 3 and 10 $ppmv$ for the same level. The thermodynamic profiles (temperature and humidity) used in this study, are provided by the global NWP model ARPEGE.

Channel number	Wavenumber [cm^{-1}]	Channel number	Wavenumber [cm^{-1}]
1479	*1014,50*	1587	*1041,50*
1509	*1022,00*	1626	*1051,25*
1513	*1023,00*	1639	*1054,50*
1521	*1025,00*	1643	*1055,50*
1536	*1028,75*	1652	*1057,75*
1574	*1038,25*	1658	*1059,25*
1579	*1039,50*	1671	*1062,50*
1585	*1041,00*		

Table 1: Wavenumber of the 15 ozone-sensitive IASI channels available in the Météo-France 314 channel subset.

Temperature, humidity and ozone data were measured using radiosondes from the collection of the World Ozone and Ultraviolet Data Center (WOUDC; available online at http://www.woudc.org), the Southern Hemisphere Additional Ozonesondes (SHADOZ; available online at croc.gsfc.nasa.gov/shadoz/Archive.html) and the National Oceanic and Atmospheric Administration (NOAA)/Earth System Research Laboratory (ESRL), Global Monitoring Division [(GMD), formerly known as the Climate Monitoring and Diagnostics Laboratory (CMDL) networks (available online at ftp://ftp.cmdl.noaa.gov/ozwv/ozone/)] as verification data to compare background and retrieval profiles. After screening to remove erroneous profiles, we were left with data from 45 stations and 1688 profiles. 394 profiles covering the Poles between (90°N, 60°N) and (60°S, 90°S), 943 profiles for the Mid latitudes between (60°N, 30°N) and (30°S, 60°S) and 351 profiles for the Tropics between (30°N, 30°S) for over a one year period from April 2014 to March 2015. It is important to noteworthy that the radiosondes provide data only up to 10 hPa.

Similar features in terms of biases are noticed for all latitudes with profiles from MOC60L (see Figure 2.a,b and c). Indeed, MOC60L underestimates ozone between 300 and 25 hPa and overestimates it above 25 hPa. The bias of RCLIM with respect to SONDE behaves differently

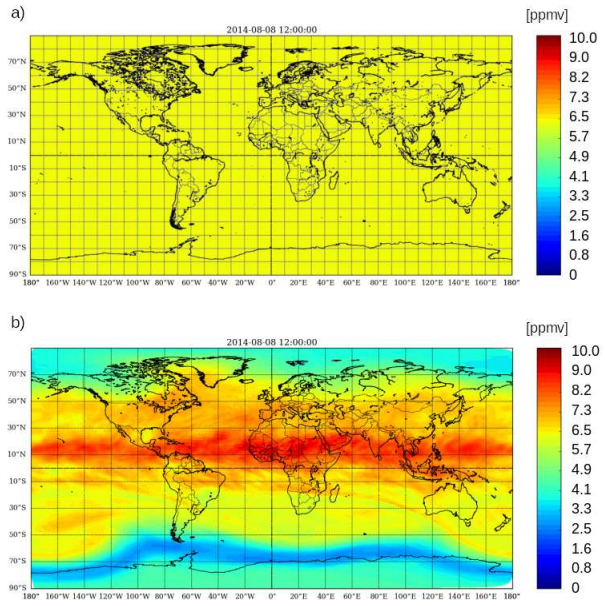

Figure 1: Example of ozone field at a particular level pressure (20 hPa) for RCLIM (a) and MOC60L (b) on 2014-08-08 at 12 UTC.

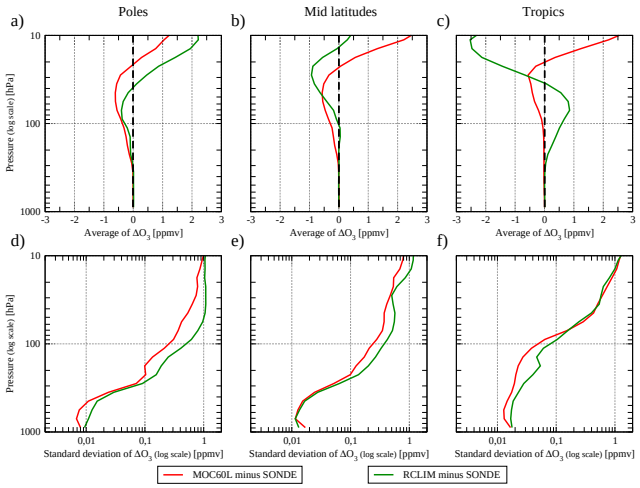

Figure 2: Average of ozone differences (RCLIM (green line) or MOC60L (red line)) minus SONDE over the Poles (a), the Mid latitudes (b) and the Tropics (c). Standard deviation of ozone differences (RCLIM (green line) or MOC60L (red line)) minus SONDE over the Poles (d), the Mid latitudes (e) and the Tropics (f).

with latitudes compared to MOC60L. In Polar regions (see Figure 2.a), RCLIM underestimates ozone between 300 and 40 hPa and overestimates it above 40 hPa. In Mid latitudes (see Figure 2.b), RCLIM overestimates ozone between 200 and 100 hPa and above 15 hPa but underestimates ozone between 100 and 15 hPa. Finally, in the Tropics (see Figure 2.c), RCLIM underestimates ozone between 300 and 30 hPa and overestimates above 30 hPa. At the Poles and for the whole atmospheric column, except at the surface, the standard deviation is lower for MOC60L than for RCLIM (see Figure 2.d). The same trend at all latitudes is observed with a lower standard deviation in the troposphere than in the stratosphere with MOC60L, which indicates a better simulation of the ozone variability in the lower atmosphere. Similar results are obtained for the Mid latitudes (see Figure 2.e) and the Tropics (see Figure 2.f). These results confirm that MOC60L better describes the variability of ozone than the constant profile of RCLIM.

In order to collocate IASI pixels and radiosondes, several criteria have been defined to select the closest pixel for each radiosonde over the period between April 2014 and March 2015. The smallest orthodromic distance and temporal difference between IASI pixel and radiosonde were retained. To avoid the use of cloudy pixels in the retrievals, IASI pixels were discarded whenever the AVHRR cloud cover was above 15 %. AVHRR is a multi-purpose imaging instrument which is used for global monitoring of cloud cover, sea surface temperature, ice, snow and vegetation cover characteristics. This instrument is an across track scanner that senses the Earth's outgoing radiation from horizon to horizon in six channels (three solar channels in the visible-near infrared region and three thermal infrared channels), with a spatial resolution of 1km at nadir and supports the IASI mission with sounding geolocation; cloud characterisation within the IASI FOV, and support to scene inhomogeneity quantification for the correction of the IASI spectral response [EUMETSAT]. To avoid emissivity and surface temperature problem, only pixels over sea with less than 10 % of land fraction were retained. Indeed, sea surface temperatures are known to be more accurate than land surface temperatures, and the RTTOV RTM includes a surface emissivity model (ISEM) [Islam et al.,] over sea. Only the pixels nearest to radiosondes are selected from those within an orthodromic distance below 150 km and a temporal difference below 60 minutes.

Therefore, 42 clear observations are collocated with radiosondes for the Poles, 71 for the Mid latitudes and 63 for the Tropics. For both RTM and 1D-Var experiments, IASI pixels were collocated within three latitudes bands. Profiles with an innovation larger than (in absolute value) 5 K were rejected. Hence, the 161 remaining pixels were divided into: 32 clear pixels over sea in the Poles; 68 clear pixels over sea in the Mid latitudes; 61 clear pixels over sea in the Tropics. The sensitivity of brightness temperature simulations to both RCLIM and MOC60L ozone fields is assessed. Temperature, humidity and surface parameters are taken from ARPEGE. The scan geometry is consistent with that of the IASI instrument. Average and standard deviations of brightness temperature differences between IASI observations and simulations [O-B], where [O-B] rep-

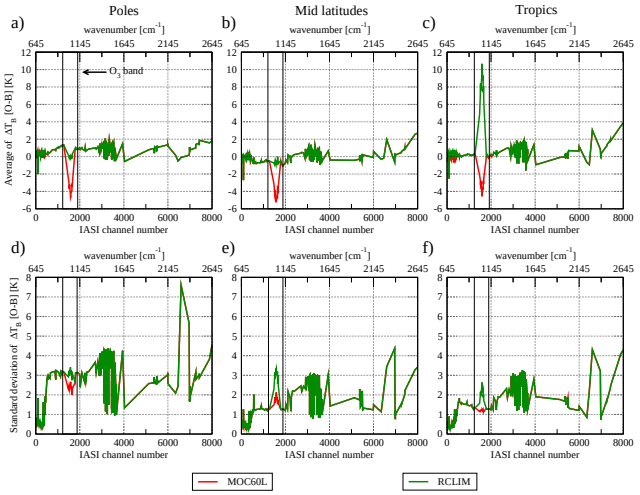

Figure 3: Average (first row) and standard deviation (Second row) of brightness temperature (BT) differences between real observations and simulations [O-B] with RCLIM (green line) and MOC60L (red line) ozone fields for IASI channels for the Poles (a and d), the Mid latitude (b and e) and the Tropics (c and f) with respect to IASI channel number and wavenumber (operationnal 314-subset).

resents the innovation d_o^b, are displayed in Figure 3. As expected differences are mainly located in the ozone band between 1014.5 and 1062.5 cm^{-1} . A consistent bias for MOC60L with values around -5 K over all regions is observed. On the other hand the RCLIM ozone bias remains low over the Poles (-0.2 K) and the Mid latitudes (-0.4 K) but is very high over the Tropics around 10 K. This bias is explained by an erroneous representativeness of the RCLIM ozone fields over the Tropics. RCLIM standard deviations for the ozone band are relatively similar over the Poles (Figure 3.d) and the Mid latitude (see Figure 3.e), with values around 3.5 K. Over the Tropics (see Figure 3.f) a lower bias around 2.5 K is found. The CO_2 channels appear to be sensitive to ozone between 650 cm^{-1} and 800cm^{-1}. Inaccurate surface temperature and the presence of sea-ice over the Poles may lead to higher standard deviations. At all latitudes, MOC60L low standard deviation values are a signature of a better representativeness of the variability than to RCLIM. These results are consistent with the differences between the climatology (RCLIM) and CTM (MOC60L).

3 Impact of ozone-sensitive channels and ozone in the control variable

Two 1D-Var assimilation experiments, with 123 IASI channels using the background ($\mathbf{x^b}$), observation ($\mathbf{y}$) data and background-error covariance matrix B were carried out following the operational Météo-France 4D-Var assimilation scheme. RDO123 and RDS123 consider a diagonal observation-error covariance matrix called $\mathbf{R_{diag}}$ with variances from respectively σ_{ope} the operational observation errors in ARPEGE and σ_{simul} derived from the differences between simulation and observation calculated with RTM. RDO123 and RDS123 experiments allow to compare the impact of operational and diagnosed observation error on analyses $\mathbf{x^a}$ (temperature and humidity retrievals). Diagonal observation-error covariance matrices only give a narrow description of the observation error. On the other hand background and observation-error covariance matrices can be estimated in observation space [Desroziers et al., 2005] from departures of observations to background and analysis. These diagnosed matrices allow to investigate if the "a priori" prescribed matrices, before analysis, are correctly specified. These revised matrices can be used for a new series of 1D-Var (a sketch of this implementation is given in Figure 4). This iterative method provides an updated version of the observation-error covariance matrix $\mathbf{R_{iter}}$. A set of 10 diagnostic iterations has been carried out. The updated $\mathbf{R_{iter}}$ matrix allows to calculate a new analysis $\widetilde{\mathbf{x}^a}$. For these experiments named RIS123, we used the same IASI observations, background profiles and background-error covariance matrix as previously done with experiment RDS123. Then, we have carried out additional experiments using the operational method RDO138 and RDS138 with respectively variance from (σ_{ope} of 123 IASI channels + σ_{simul} of 15 ozone-sensitive channels) and (σ_{simul} of 138 IASI channels) and the iterative method RIO138 and RIS138 with respectively variance from (σ_{ope} of 123 IASI channels + σ_{simul} of 15 ozone-sensitive channels) and (σ_{simul} of 138 IASI channels). Finally, the most realistic scheme (iterative method) was used to evaluate the impact of assimilating 138 channels and adding ozone in the control variable (RIS138O3).

Both the impacts of adding ozone-sensitive channels and including the ozone concentration in the control variable of the 1D-Var are evaluated. Figure 5 shows the relative improvement brought by RIS138 and RIS138O3 compared to RIS123 for temperature with respect to pressure up to 10 hPa and humidity with respect to pressure up to 100 hPa using ozone information from MOC60L or RCLIM. These statistics have been calculated for the 161 profiles. Negative values mean that retrievals from RIS138 or RIS138O3 are worse than RIS123 (-). Conversely, positive values mean that retrievals from RIS138 or RIS138O3 are better than RIS123 (+).

Almost the same results are observed with RCLIM ozone information (Figure 5.c) for retrievals from RIS138 except in the lower troposphere. A relative improvement for humidity from RIS138 retrievals using MOC60L ozone information compared to RIS123 is observed. Results in Figure 5.b show alternate improvements and degrada-

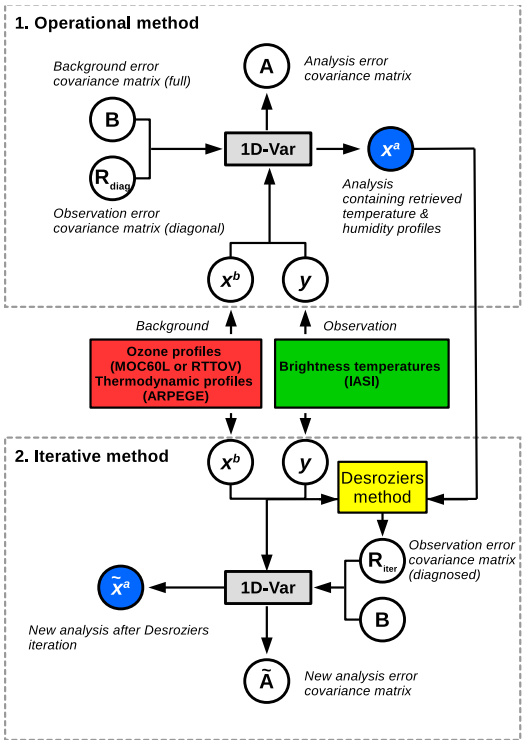

Figure 4: Scheme of operational 1D-Var methodology and Desroziers diagnostic.

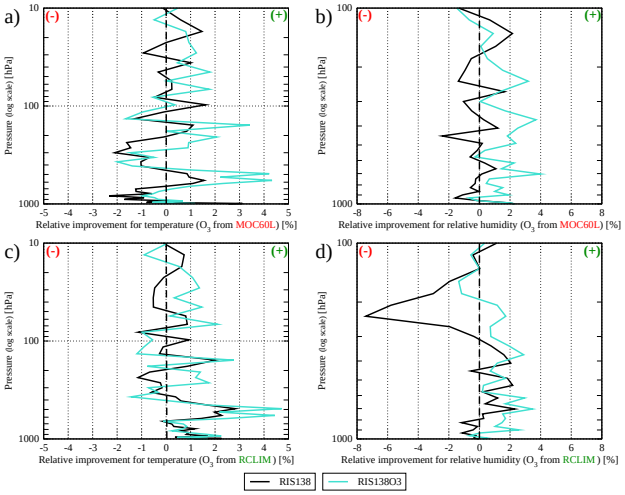

Figure 5: Relative improvement between **RIS138** (black lines) and **RIS138O3** (turquoise lines) experiments with respect to pressure until 10 hPa with ozone information from MOC60L for temperature (a) and humidity (b); and with ozone information from RCLIM for temperature (c) and humidity (d).

tions. A large degradation of retrievals from RIS138 compared to RIS123 around 200 and 300 hPa with RCLIM ozone information is noticed in Figure 5.d. These results for RIS138 experiments compared to RIS123 show that adding ozone-sensitive channels leads to gain information on atmospheric levels which are not probed by operational channels. But, we note that improvement induced by the 15 ozone-sensitive channels may also need realistic ozone information such as MOC60L from CTM MOCAGE because a non-realistic ozone field such as RCLIM, can aliase in error into temperature or humidity retrievals.

In RIS138O3 experiment, ozone was added to the control variable using the extanded background error covariance matrix. A positive impact of RIS138O3 compared to RIS138 for temperature and humidity is noticed. Indeed, having ozone in the control variable allows to gain most information from 15 ozone-sensitive channels. Whatever the ozone a priori information, ozone in the control variable allows to minimize ozone sensitive channels throughout the assimilation process. Ozone-sensitive channels are more efficient when ozone is added to the control variable for improving the thermodynamic retrievals.

To summarize the results of the main experiments, Table 2 shows the percentage of the averaged error reduction weighted by the number of profiles for temperature AVG_T, humidity AVG_Q and AVG_{O_3}:

$$AVG_T = \frac{\frac{1}{n_p}\sum_{r\in lat} RED_{T,r} * n_r}{\sum_{r\in lat} n_r}$$

$$AVG_Q = \frac{\frac{1}{n_p}\sum_{r\in lat} RED_{Q,r} * n_r}{\sum_{r\in lat} n_r}$$

$$AVG_{O_3} = \frac{\frac{1}{n_p}\sum_{r\in lat} RED_{O_3,r} * n_r}{\sum_{r\in lat} n_r}$$

RED_T, RED_{O_3} and RED_Q represents respectively the reduction of error for temperature, ozone and humidity, n_p, the vertical levels (54 for temperature, 29 for humidity), r, the considered latitude bands (Poles, Mid-latitudes and Tropics) and n_r is number of profiles by latitudes. Positive (resp. negative) AVG values mean a degradation (resp. an improvement) of retrievals for all latitudes.

$$RED_T = \sum_{i=1}^{n_T}\left[\frac{sd(\mathbf{x}_i^a - \mathbf{x}_i^v) - sd(\mathbf{x}_i^b - \mathbf{x}_i^v)}{sd(\mathbf{x}_i^b - \mathbf{x}_i^v)}\right]$$

$$RED_Q = \sum_{i=1}^{n_q}\left[\frac{sd(\mathbf{x}_i^a - \mathbf{x}_i^v) - sd(\mathbf{x}_i^b - \mathbf{x}_i^v)}{sd(\mathbf{x}_i^b - \mathbf{x}_i^v)}\right]$$

$$RED_{O_3} = \sum_{i=1}^{n_{O_3}}\left[\frac{sd(\mathbf{x}_i^a - \mathbf{x}_i^v) - sd(\mathbf{x}_i^b - \mathbf{x}_i^v)}{sd(\mathbf{x}_i^b - \mathbf{x}_i^v)}\right]$$

Ozone from	MOC60L		
[%]	AVG_T	AVG_Q	AVG_{O_3}
RDO123	+2.48	+5.15	
RIS123	-2.51	-5.15	
RIS138	-2.37	-5.67	
RIS138O3	-2.63	-6.22	-0.59
Ozone from	RCLIM		
[%]	AVG_T	AVG_Q	AVG_{O_3}
RDO123	+2.86	+5.87	
RIS123	-2.48	-5.07	
RIS138	-2.83	-4.48	
RIS138O3	-2.82	-6.07	-0.17

Table 2: Error reduction [%] averaged over profiles and vertical levels (positive impact if negative value).

Using the standard deviation (sd), at each vertical level i, n_T and n_{O_3} being the number of 54 vertical temperature levels and n_q being the number of 29 vertical levels for humidity, of:

- $\mathbf{x}_i^a$ or $\widetilde{\mathbf{x}_i^a}$: retrieval from respectively operational or iterative method minus $\mathbf{x}_i^v$ (verification data from radiosondes);
- $\mathbf{x}_i^b$: background minus $\mathbf{x}_i^v$.

With the operational method, AVG values (temperature and humidity) are degraded, independently of the source of ozone information. The mean degradation exceeds 2 % for temperature and 5 % for humidity. The iterative method improves AVG values by more than 2 % for temperature and 5 % for humidity. The impact of the 15 additional ozone-sensitive channels varies with the ozone information. AVG_Q values in RIS138 using MOC60L are improved, less so for AVG_T ones, but it is the reverse for RIS138 using RCLIM. As temperature and humidity are affected when ozone is absent from the control variable, its addition the RIS138O3 experiment improved both AVG_T and AVG_Q. The ozone changes during the assimilation process, which allows to correct the error of ozone fields and avoid aliasing ozone error information on temperature or humidity. Retrievals are improved by about 2.5 % for temperature and 6 % for humidity compared to background. In addition, we note an improvement by about 0.6 % for ozone using a prior ozone information from MOC60L and 0.2 % using ozone from RTTOV compared to background. Using observation errors from simulations combined with the Desroziers' diagnostic method, plus the addition of ozone-sensitive channels and ozone in the control vector lead to improved thermodynamic retrievals.

4 Conclusions and discussions

The prime aim of this study was to add information on atmospheric composition for the assimilation of radiances from the IASI infrared sounder in the global NWP model ARPEGE (which uses some gases that do not vary neither in time nor in space). More precisely, we wanted to improve thermodynamics retrievals and forecasts by the addition of ozone-sensitive channels. At present, Météo-France 4D-Var (Four dimensional variational data assimilation) assimilation system uses only 123 IASI channels out of 314 monitored operationaly. We have investigated within a simplified framework such as the one dimensional variational data assimilation because of its low computing cost.

This study has shown that using a realistic ozone information from CTM into RTM allows to better simulate IASI radiances and thus to diagnose more optimal observation errors σ_{simul} compared to those used operationally. It is already interesting to use diagnosed observation errors within a diagonal observation-error covariance matrix. The use of a more optimal observation-error covariance matrix calculated from the Desroziers method shows an additional improvement of thermodynamic retrievals with 123 operational channels. The addition of 15 ozone-sensitive channels provides information on the lower troposphere and the stratosphere previously uncovered in temperature and humidity. However, error in ozone information can affect temperature and humidity retrievals. Thermodynamic profiles from ARPEGE show an important bias in the troposphere. Hence, the expected precision of IASI for humidity (10 %/1 km) is not met. Finally, the study shows that, realistic ozone information from CTM is important if ozone-sensitive channels are added without ozone in the control variable. However, when ozone is included in the control variable, adding ozone-sensitive channels allows to improve further thermodynamics and chemical retrievals. In order to overcome interactions between IASI measurements and clouds and emissivity of land surfaces, we have only used clear-sky pixels over sea. However, these area are poor in radio-sounding and thus it might be interesting to assess impact of assimilation experiments with ozone-sensitive channels over the land or in cloudy conditions. Though 15 ozone-sensitive channels from Collard's selection were used, it may be more efficient to identify other sensitive channels from the 8461 available channels. Realistic ozone profiles from radio-sounding for the same IASI collocated pixels were used. As radio-soundings are not available above 10 hPa, thermodynamic and ozone information from MOC60L were added.

The Copernicus Atmosphere Monitoring Service (CAMS) programme provides forecasts of different gases, especially greenhouse gases. It would be of interest to use more realistic information sources for CO_2 for example, in assimilation and used in conjunction with realistic ozone information and this paves the way to similar studies with future sensors such as IASI-NG, [Crevoisier et al., 2014] which will have 16921 channels. Further studies should

include CO, CH_4, N_2O and many more. Furthermore, we started to assess the forecast impact of additional ozone-sensitive channels using ozone information from MOCAGE and add the ozone in the ARPEGE 4D-Var control variable. The same approach as in the 1D-Var experiment is used. The first step of results are very promising and will be the subject of an upcoming article.

Acknowledgements

Olivier Coopmann's PhD is funded by CNES and Région Occitanie

References

[Cayla, 2001] Cayla, F.-R. (2001). L'interféromètre iasi-un nouveau sondeur satellitaire haute résolution.

[Chevallier et al., 2006] Chevallier, F., Di Michele, S., and McNally, A. P. (2006). *Diverse profile datasets from the ECMWF 91-level short-range forecasts*. European Centre for Medium-Range Weather Forecasts.

[Clerbaux et al., 2009] Clerbaux, C., Boynard, A., Clarisse, L., George, M., Hadji-Lazaro, J., Herbin, H., Hurtmans, D., Pommier, M., Razavi, A., Turquety, S., et al. (2009). Monitoring of atmospheric composition using the thermal infrared iasi/metop sounder. *Atmospheric Chemistry and Physics*, 9(16):6041–6054.

[Collard, 2007] Collard, A. (2007). Selection of iasi channels for use in numerical weather prediction. *Quarterly Journal of the Royal Meteorological Society*, 133(629):1977–1991.

[Courtier et al., 1994] Courtier, P., Thépaut, J.-N., and Hollingsworth, A. (1994). A strategy for operational implementation of 4d-var, using an incremental approach. *Quarterly Journal of the Royal Meteorological Society*, 120(519):1367–1387.

[Crevoisier et al., 2014] Crevoisier, C., Clerbaux, C., Guidard, V., Phulpin, T., Armante, R., Barret, B., Camy-Peyret, C., Chaboureau, J.-P., Coheur, P.-F., Crépeau, L., et al. (2014). Towards iasi-new generation (iasi-ng): impact of improved spectral resolution and radiometric noise on the retrieval of thermodynamic, chemistry and climate variables. *Atmospheric Measurement Techniques*, 7:4367–4385.

[Desroziers et al., 2005] Desroziers, G., Berre, L., Chapnik, B., and Poli, P. (2005). Diagnosis of observation, background and analysis-error statistics in observation space. *Quarterly Journal of the Royal Meteorological Society*, 131(613):3385–3396.

[Hilton et al., 2012] Hilton, F., Armante, R., August, T., Barnet, C., Bouchard, A., Camy-Peyret, C., Capelle, V., Clarisse, L., Clerbaux, C., Coheur, P.-F., et al. (2012). Hyperspectral earth observation from iasi. *bulletin of the american meteorological Society*, 93(3):347.

[Islam et al.,] Islam, T., Srivastava, P. K., and Petropoulos, G. P. Uncertainty quantification in the infrared surface emissivity model (isem).

[Lorenc and Marriott, 2014] Lorenc, A. C. and Marriott, R. T. (2014). Forecast sensitivity to observations in the met office global numerical weather prediction system. *Quarterly Journal of the Royal Meteorological Society*, 140(678):209–224.

[Martinet et al., 2014] Martinet, P., Lavanant, L., Fourrié, N., Rabier, F., and Gambacorta, A. (2014). Evaluation of a revised iasi channel selection for cloudy retrievals with a focus on the mediterranean basin. *Quarterly Journal of the Royal Meteorological Society*, 140(682):1563–1577.

[Saunders and Kriebel, 1988] Saunders, R. W. and Kriebel, K. T. (1988). An improved method for detecting clear sky and cloudy radiances from avhrr data. *International Journal of Remote Sensing*, 9(1):123–150.

[Sic et al., 2015] Sic, B., El Amraoui, L., Marécal, V., Josse, B., Arteta, J., Guth, J., Joly, M., and Hamer, P. (2015). Modelling of primary aerosols in the chemical transport model mocage: development and evaluation of aerosol physical parameterizations. *Geoscientific Model Development*, 8(2).